ELSEVIER

Journal of Nuclear Materials 271&272 (1999) 15–20

journal of nuclear materials

Radiation effects of 200 keV and 1 MeV Ni ion on MgO single crystal

T. Mitamura [a], K. Kawatsura [b,*], R. Takahashi [b], T. Adachi [b], T. Igarashi [b], S. Arai [b], N. Masuda [b], Y. Aoki [c], S. Yamamoto [c], K. Narumi [c], H. Naramoto [c], Y. Horino [d], Y. Mokuno [d], K. Fujii [d]

[a] *Faculty of Engineering, Himeji Institute of Technology, Himeji, Hyogo 671-2201, Japan*
[b] *Department of Chemistry and Materials Technology, Faculty of Engineering and Design, Kyoto Institute of Technology, Goshokaido-cho, Matsugasaki, Sakyo, Kyoto 606-8585, Japan*
[c] *Japan Atomic Energy Research Institute, Takasaki, Gunma 370-1208, Japan*
[d] *Osaka National Research Institute, AIST, Ikeda, Osaka 563, Japan*

Abstract

Effects of Ni ion implantation on MgO (1 0 0) single crystals were examined by Rutherford backscattering spectrometry with channeling and optical absorption measurements. Ni ions with energy of 1.0 MeV and 200 keV were implanted at room temperature in the dose range, 1×10^{15}–1×10^{17} cm^{-2}. By applying thermal annealing method, recovery of the radiation induced damage was followed and the distribution and lattice location of implanted Ni ions was analyzed. It was observed that the radiation induced defects in the as-implanted sample were formed near Ni ion distribution, which is different from the theoretical prediction by the E-DEP-1 code. After thermal annealing above 500°C, defects began to recover, and rapid recovery of the lattice order and simultaneous diffusion of implanted Ni were observed above 1100°C until they reach full recovery at 1400°C. A part of these changing phenomena was supported by the optical absorption measurements.

1. Introduction

Ceramics are important candidate materials for fusion reactor applications while in many other fields new ceramic materials are expected to be developed. It is important to understand growth and annihilation process of radiation defects, since desirable physical properties of ceramics are kept unchanged, or are prolonged, under the environment of high energy particle irradiation. In addition, ion implantation is one of the important techniques in the field of modification of ceramics/insulator materials. There have been a number of studies of MgO single crystals implanted with various ions, i.e. energetic electrons, light atoms, alkali metal atoms, rare gas atoms, transition metal atoms and other metals [1–11]. For ceramic materials such as Al_2O_3, CaO and MgO, radiation-induced color centers play an important role especially in the modification of properties of ceramics/insulator materials as well as in the atomic disorder induced by ion implantation. However, few results have been reported on the simultaneous measurements of both vacancy- and displacements-type defects. In this paper, we report on the radiation effects in MgO single crystals introduced by energetic Ni ion implantation. During thermal annealing treatments, the recovery of radiation effects was followed and the relation between color centers (vacancy-type defects) and lattice disorder (atom displacement-type defects) was simultaneously analyzed using Rutherford backscattering spectrometry with channeling (RBS-C) and optical absorption spectroscopy.

* Corresponding author. Fax: +81-75 724 7210; Tel.: +81-75 724 7507; e-mail: kawatura@ipc.kit.ac.jp.

0022-3115/99/$ – see front matter
PII: S0022-3115(98)00727-2

2. Experimental

2.1. Sample preparation

The cleaved MgO(1 0 0) single crystals ($10 \times 10 \times 0.5$ mm^3) were obtained from Tateho Chemical Industries Co. The concentrations of intrinsic impurities are as follows (in ppm): Al(60), Ca(70), Cr(13), Co(3), Fe(120), Mn(9), Ni(3), and other impurities (<30 ppm in total). Using the 3 MV tandem accelerator or the 400 kV ion implanter at the TIARA facilities of JAERI, Takasaki, $^{58}Ni^+$ ions with energies of 1.0 MeV or 200 keV were implanted at room temperature in the dose range of 9.2×10^{14}–9.2×10^{16} cm^{-2}. During the ion implantation, the degree of vacuum of the target chamber was kept at about 1×10^{-5} Pa, and the beam current was kept at about 1 μA cm^{-2} in order to avoid thermal effects. The thermal treatments of the samples were performed in an atmosphere of Ar gas flow at temperatures ranging from 100°C to 1400°C for 1 h.

2.2. Measurements

RBS-C measurements were carried out so as to examine the radiation damage, the implantation profile, and the lattice location of implanted ions, using $^4He^+$ ion as a probe; 1.6–2.0 MeV $^4He^+$ ions accelerated by the 2MV van de Graaff accelerator at Osaka National Research Institute, Ikeda, and 2.5–3.0 MeV $^4He^+$ ions accelerated by the 3 MV single-ended accelerator at the TIARA facilities of JAERI, Takasaki.

In RBS-C spectroscopy, when aligning the incident ion beam with a crystal axis or plane (channeling), the channeled ions not only reduce their probability of interactions with the atomic nuclei of the crystal but also change their interaction with the electrons of the crystal, resulting in a decrease in the number of the backscattered particles. The number of the backscattered particles increase when the crystal is rotated so that the incident ions view the crystal as a random collection of atoms. These aligned yields and random yields of the backscattered He ion are used to estimate disorder of the crystal lattice. The backscattered He ion energy deposited in the detector is given by subtracting the absorbed energy from the incident He ion energy. The absorbed energy is the sum total of the energy loss due to the stopping power of target material for He ions and the transferred energy in collision between He ion and target atoms, Hence, information of the lattice disorder and the position of the target atoms in the solid is derived by RBS spectrum analysis. Details of the analyzing methods of the RBS-C spectrum can be found elsewhere [12].

For the samples implanted with 200 keV Ni ions, optical absorption spectroscopy was applied to measure color centers with the use of a spectrophotometer (Hitachi 200-20) in the wavelength range from 200 to 850 nm at room temperature. An unimplanted MgO sample served as a reference. The concentration of color centers was estimated by Dexter's form of Smakula's equation [13].

3. Results and discussion

3.1. MeV Ni ion implanted MgO(1 0 0)

3.1.1. RBS-C spectra

The random and the aligned RBS spectra for the 1.0 MeV Ni^+ ion as-implanted MgO(1 0 0) are shown in Fig. 1, together with the aligned RBS spectrum for the unimplanted region of the same sample. The implantation dose was 9.2×10^{16} cm^{-2}. These spectra were obtained with the use of 3.0 MeV He^+ ion as a probe. Arrowheads in the figure indicate the elements at surface. The minimum yield χ_{min} (the ratio of the aligned yield to the random yield) for Mg at the unimplanted region is 0.03, which means that the MgO(1 0 0) single crystalline sample is of a high enough quality to study radiation-induced effects. What is evident on comparing the two aligned spectra is that, after ion implantation, radiation induced damage is very weak at the surface region and considerable damage can be seen around the Ni ion range (~500 nm). From spectrum analysis, it is observed that 27% of the implanted Ni ions are located at the substitutional position of crystal lattice and, especially at the depth of 500 nm, 20% of them are substitutional.

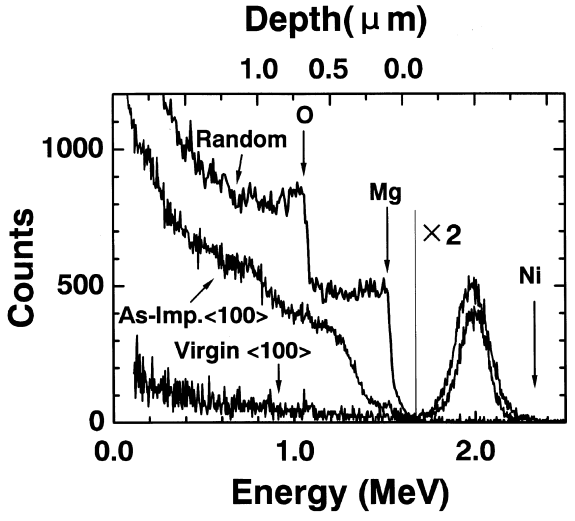

Fig. 1. RBS-C spectra for the as-implanted MgO with a dose of 9.2×10^{16} cm^{-2} of 1.0 MeV Ni^+ ions together with the aligned spectrum for unimplanted region. RBS-C spectra were measured by using 3.0 MeV He^+ ions.

Fig. 2 shows comparison of the calculated implantation profile of 1.0 MeV Ni ions and damage profile with the experimental results. The theoretical calculation was performed by using the E-DEP-1 code [14]. The implantation profile is a nearly Gaussian distribution with a maximum concentration of 4 at.% at a depth of 500 nm (see Fig. 2(a)). The full width at half maximum (FWHM) of the Ni atom profile is 340 nm for the experimental result, and 250 nm for the calculated one. No appreciable difference can be seen between the two profiles. Fig. 2(b) shows comparison of the disorder profile with the theoretically calculated dpa (displacement per atom) profile. A discrepancy exists between the two profiles. The calculated dpa at the surface, at 380 and 800 nm are 55, 104, and 0, respectively. However, amounts of the disorder for Mg atoms are 2×10^{21}, 1.8×10^{22}, and 1×10^{21} cm^{-3} at the corresponding depth. The calculated dpa has a maximum at a depth of about 380 nm and has almost the same value of 60 at 100 and 500 nm, while a large difference is observed between the amounts of disorder at these depths. The disorder at 500 nm is about one order larger than that at 100 nm. The calculated dpa at 380 nm is about twice as large as that at 500 nm, but the disorder at 380 nm is almost the same as that at 500 nm. These experimental results suggest that the disorder of Mg atoms is correlated with the distribution of the implanted Ni atoms rather than the dpa induced by incident Ni ions.

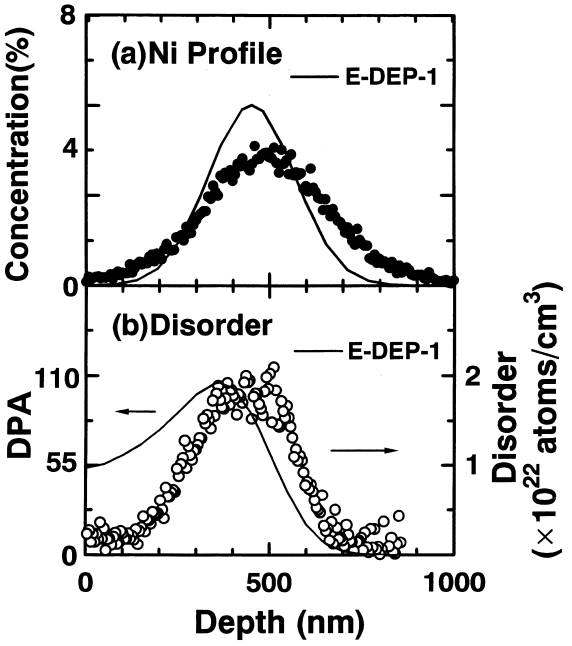

Fig. 2. Implantation profile (a) and radiation damage profile (b) for MgO(1 0 0) implanted with a dose of 9.2×10^{16} cm^{-2} of 1.0 MeV Ni$^+$ ions. Ni profile(●) and disorder profile(○) obtained for RBS-C measurement. The solid line represents calculated Ni and DPA profiles by using E-DEP-1 code.

3.1.2. Dose dependence on disorder for Mg atoms

In the case of 1.0 MeV Ni$^+$ ion implantation, the dose dependence of the disorder in the Mg sublattice at depths of 100 and 500 nm are shown in Figs. 3 and 4. The depth of 500 nm corresponds to the average range of 1.0 MeV Ni$^+$ ions. From Fig. 3, it can be seen that the disorder for the Mg atoms at 100 nm increases linearly from 0.2×10^{22} to 0.25×10^{22} cm^{-3} with increase of Ni ion implantation dose from 9.2×10^{14} to 9.2×10^{16} cm^{-2}, while, at 500 nm, the disorder rapidly increases in the initial stage of Ni ion implantation and shows the saturation trend up to a dose of 2×10^{16} cm^{-2}.

It is interesting to see Fig. 4, because the observable disorder for Mg atoms starts at a 1.0 MeV Ni ion dose of 2×10^{13} cm^{-2}. For the 200 keV Ni ion implanted sample, the disorder at a depth of 250 nm, that is the average range of implanted Ni ions, increases with the increase in ion dose and has a maximum at a dose of about 5×10^{16} cm^{-2}.

3.1.3. Annealing behavior of disorder and implanted Ni atoms

The thermal annealing behavior of radiation induced damage and implanted Ni ions was investigated. For the sample implanted with 1.0 MeV Ni ions to a dose of 9.2×10^{16} cm^{-2}, the annealing behavior of the disorder in the Mg sublattice and the substitutional fraction of Ni ions are shown in Fig. 5. The solid circle and the open square indicate the disorder in the Mg sublattice at 100 and 500 nm, respectively. The substitutional Ni fraction is indicated by a double circle. The disorder of Mg atoms at 100 nm decreases slowly with the increase in

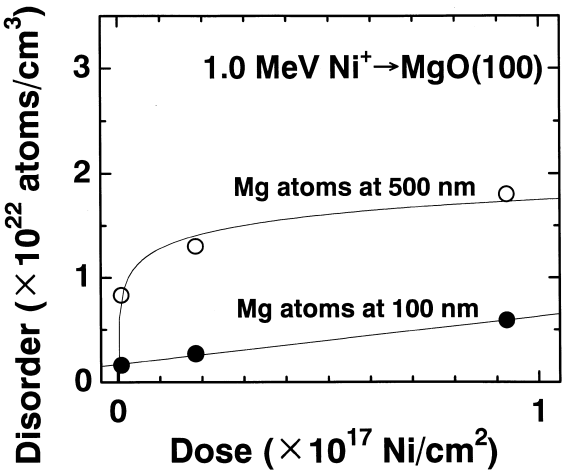

Fig. 3. The dependence of the disorder for Mg atoms on Ni ion dose in linear scale at the depth of 100 and 500 nm.

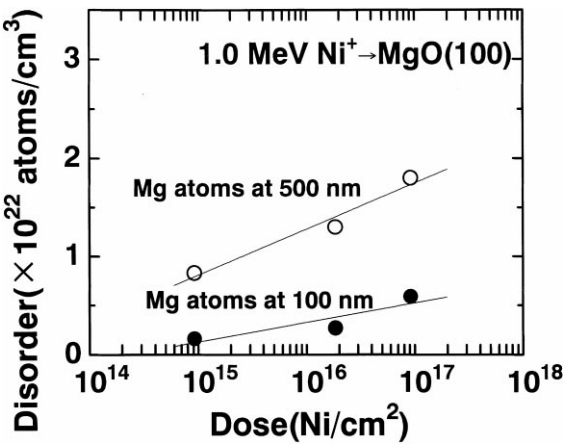

Fig. 4. The dependence of the disorder for Mg atoms on Ni ion dose in log scale at the depth of 100 and 500 nm.

annealing temperature. On the other hand, the disorder of Mg atoms at 500 nm shows no appreciable change after 500°C annealing. It decreases slowly during 500–1000°C annealing, and then it decreases sharply after 1100°C annealing. The Mg sublattice is rapidly ordering due to the redistribution of displaced Mg atoms in the cation vacancies. After annealing at 1400°C, the disorder for Mg atoms at 500 nm is completely recovered.

We compare the thermal annealing behavior for the implanted Ni ions with that for Mg at the same depth of 500 nm. After implantation, 20% of the Ni ions are located at substitutional sites. This fraction is not changed during the annealing treatments from 500°C to 800°C. But after annealing at 1000°C, the fraction decreases temporarily from 20% to 10%. This result is similar to the result obtained by Perez et al. [5]. After 1100°C annealing, the displaced Mg atoms begin to locate at MgO lattice order sites and a simultaneous increase in the fraction of the substitutional Ni ions takes place. The fraction reaches about 67% after 1200°C annealing.

Fig. 6 shows the distribution profiles of Ni atoms. In the case of the 1200°C annealing sample, the Ni ion profile cannot be totally observed because 1.8 MeV He ions were used as a probe. The Ni ions probably diffuse to the inner region with a depth in excess of 500 nm. After 1100°C annealing, the implanted Ni ions are considered to occupy substitutional sites by forming NiO, which, like MgO, has a NaCl type structure. At the same time the disorder for Mg recovers (see Fig. 5). After annealing at 1400°C, most of the implanted Ni ions diffuse to the whole region of the crystal, resulting in a low flat distribution as shown in the spectrum.

3.2. 200 keV Ni ion implanted MgO(1 0 0)

3.2.1. Optical absorption spectra

Optical absorption measurements were carried out for the 200 keV Ni implanted MgO(1 0 0) crystal. The variation of spectra with the Ni doses between 1.6×10^{15} and 8.0×10^{16} cm^{-2} is presented in Fig. 7. The absorption band at near 250 nm is identified with an F-type center. Krappers et al. [15] have shown that the 250 nm absorption band is composed of two close bands, i.e. an F center (246.5 nm), and F^+ center (250.0 nm). A V^- center (570 nm), F_2 center (350 nm), and Fe^{3+} impurity center (220 nm) are observed. The spectra show F-type and V^- centers increase with the increase of Ni ion dose, and aggregate centers appear at a high Ni ion dose.

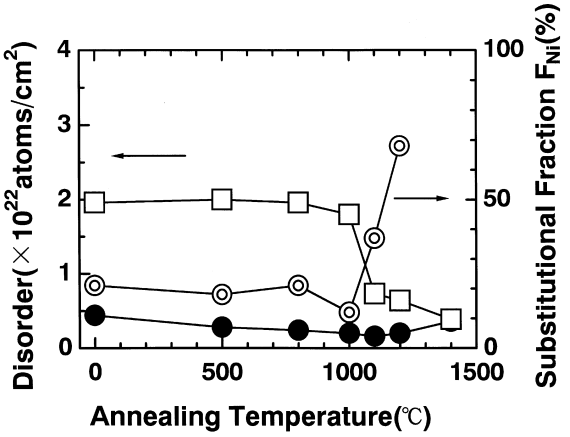

Fig. 5. The disorder in the Mg sublattice at a depth of 100 nm (●) and 500 nm (□), and the substitutional fraction of Ni ions at a depth of 500 nm (●) after thermal annealing treatments for MgO(1 0 0) implanted with a dose of 9.2×10^{16} cm^{-2} of 1.0 MeV Ni^+ ions.

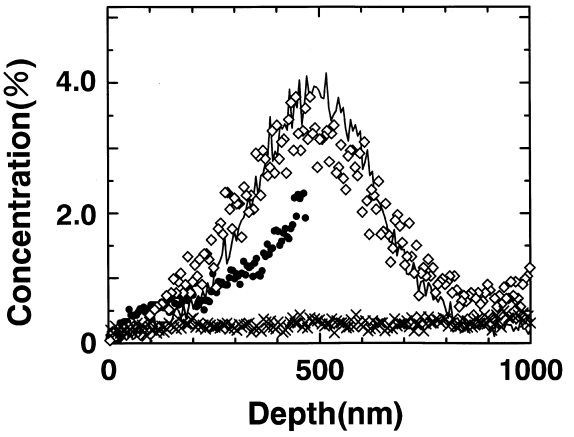

Fig. 6. The implantation profile of MgO(1 0 0) implanted with a dose of 9.2×10^{16} cm^{-2} of 1.0 MeV Ni^+ ions after thermal annealing. The solid line gives the Ni profile of as H implanted sample: 1100°C annealing (◇), 1200°C annealing (●) and 1400°C annealing (×).

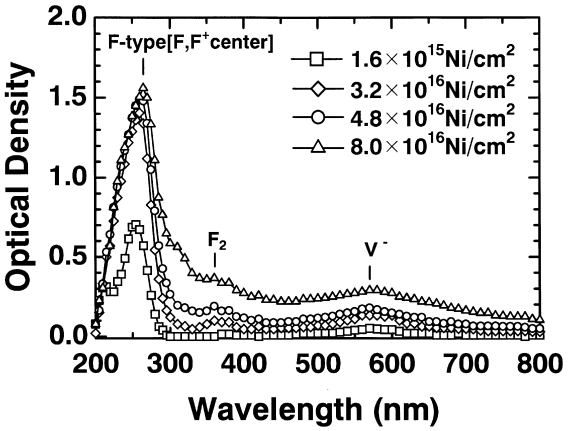

Fig. 7. The optical absorption spectra of MgO(1 0 0) implanted with 200 keV Ni^+ ions and doses of: 1.6×10^{15} cm^{-2} (□), 3.2×10^{16} (◇), 4.8×10^{16} (○) and 8.0×10^{16} (△).

3.2.2. Dose dependence and annealing behavior of vacancy type defects

Using the Dexter's formula of Smakula [13], the concentrations of F-type and V^- centers are estimated in Fig. 8. The concentration of both centers increases with an increase in the dose and reach maximum values for a dose of around 5×10^{16} ions/cm^2 and then decreases above it. At the maximum, the concentration of F-type and V^- centers are 4.8×10^{21} and 6.5×10^{20} cm^{-3}, respectively. This tendency was also observed, not shown here, in the dose dependence of the disorder for Mg atoms obtained by RBS-C for 200 keV Ni implanted samples. Previous results also show the same tendency that the concentration of the both F-type and V^- centers increases with an increase in the dose and reach a maximum for a dose of around $2–4 \times 10^{16}$ cm^{-2} and decrease above it [3–5].

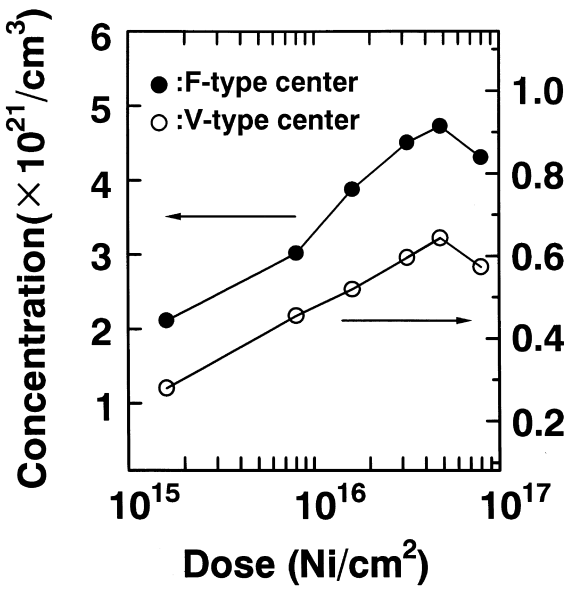

Fig. 8. The concentration of F-type (●) and V^- center (○) of MgO(1 0 0) implanted with 200 keV Ni^+ ions to a dose from 1.6×10^{15} to 8.0×10^{16} cm^{-2}.

The annealing behavior of the optical absorption spectra were measured for Ni implanted MgO samples at temperatures between 300°C and 500°C. The F-type centers start to vanish after 500°C and the V^- center, after 400°C annealing. The F^{2+} center (470 nm) and Fe^{3+} absorption band (310 nm) increase sharply from 300°C and reach the saturation level, while the disorder for Mg atoms measured by RBS-C did not change.

4. Conclusion

An MgO(1 0 0) single crystal was implanted with 1.0 MeV and 200 keV Ni ions and the various induced effects were studied by RBS-C and optical absorption measurements. The lattice disorder induced by 1.0 MeV Ni implantation was strongly correlated with the distribution of the implanted Ni ions. After thermal annealing above 1100°C, Ni atoms began to locate at substitutional lattice position forming NiO and diffuse. The radiation induced effects were recovered after 1400°C annealing. Color centers induced by 200 keV Ni ion implantation were assigned as F-type and V^- centers by optical absorption measurements. Implantation dose dependence of the color center concentration shows a similar tendency to the results obtained by RBS-C measurements.

Acknowledgements

The authors wish to thank Dr T. Aruga for his calculations of E-DEP-1 code. This work was supported in partly by the JAERI-TIARA cooperative program.

References

[1] B.D. Evans, Phys. Rev. B 9 (1974) 5222.
[2] Hj. Matzke, A. Tuos, P. Rabette, O. Meyer, J. Phys. C 14 (1981) 3333.
[3] A. Perez, M. Treilleux, P. Thevenard, G. Abouchacra, G. Marest, L. Fritsch, J. Serughetti, Metastable Materials Formation by Ion Implantation, Elsevier, Amsterdam, 1982, p. 159.
[4] A. Peretz, G. Marest, B.D. Sawicka, J.A. Sawicki, T. Tyliszczak, Phys. Rev. B 28 (1983) 1227.
[5] A. Perez, M. Treilleux, L. Fritsch, G. Marest, Radiat. Eff. 64 (1982) 199.
[6] G. Fuchs, G. Abouchacra, M. Treilleux, P. Thevenard, J. Serughetti, Nucl. Instrum. Meth. B 32 (1988) 100.

[7] W.R. Allen, S.J. Zinkle, J. Nucl. Mater. 191/194 (1992) 625.
[8] E. Friedland, M. Hayes, Nucl. Instrum. Meth. B 65 (1992) 287.
[9] E. Friedland, Nucl. Instrum. Meth. B 85 (1994) 316.
[10] S.J. Zinkle, Nucl. Instrum. Meth. B 91 (1994) 234.
[11] T. Futagami, Y. Aoki, O. Yoda, S. Nagai, Nucl. Instrum. Meth. B 88 (1994) 261.
[12] W.-K. Chu, J.W. Mayer, M.-A. Nicolet, Backscattering Spectroscopy, Academic Press, San Diego, CA, 1978.
[13] D.L. Dexter, Phys. Rev. 101 (1956) 48.
[14] I. Manning, G.P. Mueller, Comput. Phys. Commun. 7 (1974) 85.
[15] L.A. Kappers, R.L. Kroes, E.B. Hensley, Phys. Rev. B 1 (1970) 4151.